Materials & Design 208 (2021) 109910

Contents lists available at ScienceDirect

Materials & Design

journal homepage: www.elsevier.com/locate/matdes

Corrosion prediction for bulk carrier via data fusion of survey and experimental measurements

Z. Wang [a], A.J. Sobey [a,b], Y. Wang [a,*]

[a] Maritime Engineering Group, University of Southampton, Southampton, UK
[b] Marine and Maritime Group, Data-centric Engineering, The Alan Turing Institute, The British Library, London, UK

HIGHLIGHTS

- Develop a new artificial neural network-based data fusion model to provide tailored corrosion predictions for bulk carriers.
- Combine operational information from ship surveys and corrosion fundamentals from experimental measurements.
- Prediction accuracy is improved by at least 82% compared to the state-of-the-art corrosion models.
- The model quantifies the contribution of different environmental/operating factors to the marine corrosion of carbon steels.

GRAPHICAL ABSTRACT

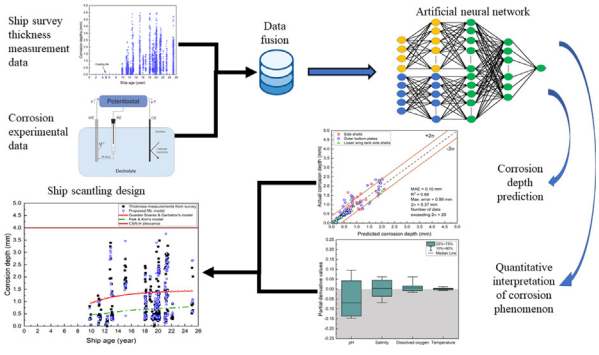

ARTICLE INFO

Article history:
Received 4 April 2021
Revised 1 June 2021
Accepted 16 June 2021
Available online 19 June 2021

Keywords:
Carbon steels
Immersion and atmospheric corrosion
Artificial neural network
Interpretable machine learning
Marine environments
Bulk carrier ballast tanks

ABSTRACT

Accurate corrosion predictions are vital to safe and optimised designs of marine assets. Traditional approaches, including those used to develop rule requirements, seek to use empirical regressions to model corrosion, but most are solely time-dependent. This may lead to conservative damage estimates and hence heavy and inefficient ships. To provide more accurate predictions, this paper presents an interpretable machine learning algorithm based on data fusion of ship survey and experimental measurements. The corrosion behaviour in bulk carrier ballast tanks is interpreted through a sensitivity analysis which quantifies the relationships between operational/environmental factors and the corrosion rate. The prediction accuracy is improved by a minimum of 82% when compared to the two representative empirical models, with a mean absolute error down to 0.10 mm.

1. Introduction

Marine corrosion of carbon steels has been extensively investigated. However, to accurately predict the corrosion rate of ocean-going ships, more than 90% of which are made of carbon steels, remains one of the most challenging tasks in materials science and maritime engineering [1]. This is because ships operate under complex conditions for an extensive period of time (typically more than 25 years). For example, bulk carriers, one of the major commercial ship types, show complex corrosion phenomena in ballast water tanks, decks and cargo holds (depending on the corrosivity of the cargos). More details regarding corrosion predictions are available in the authors' review [2]. From this review it is found that some of the empirical models in the literature are able to predict the general trends in corrosion and thickness reductions. How-

* Corresponding author.
E-mail address: Yikun.Wang@soton.ac.uk (Y. Wang).

https://doi.org/10.1016/j.matdes.2021.109910
0264-1275/

ever, they cannot predict the thickness change on an individual plate, which varies greatly across a ship due to different operating conditions.

Fig. 1 summarises the main influencing factors of ship corrosion, which can be broadly categorised as ship operating factors and environmental factors. Research on the environmental factors is focused on understanding the degradation mechanisms and kinetics in a particular corrosive environment, mainly using experimental methods. Table 1 categorises the available experiments for immersion corrosion in seawater and atmospheric corrosion in coastal/harbour areas for carbon steels. Studies on the immersion corrosion includes the effects of the short-term (less than 6 months) immersion in seawater [3,4], long-term immersion conditions, rust layer formations [5,6], anaerobic/aerobic conditions [7,8], the roles of cathodic protections [4,9–12] and different types of inhibitors [4,13–20]. The focus of the current atmospheric corrosion experiments is the analysis of corrosion products and the effects of environmental conditions, especially the influences of airborne deposits [21–23]. The measurements are relevant to the corrosion of ship ballast tanks and external hulls (decks, side shells and bottom shells). However, they cannot be directly utilised to predict the corrosion rate.

For practical engineering applications, survey data is used instead to predict corrosion depths/rates, traditionally through probabilistic models and more recently through regression [2]. The probabilistic modelling approach was used by the International Association of Classification Societies (IACS) by defining corrosion diminution at 95% cumulative probability for 25 years to develop the design corrosion allowances for bulk carriers and tankers. The majority of the empirical regression models are only time-dependent. For example, the model developed by Paik and Kim [52] for bulk carrier ballast tanks used the thickness measurement data collected from periodical surveys and a regression line to represent the relationship between the corrosion depth/rate and ship age. The Weibull function is considered to best represents the distribution of carbon steel corrosion in ballast tanks. In comparison, Guedes Soares and Garbatov [53] show that the corrosion rate would gradually approach zero after long-term exposure, due to the oxide layer. Therefore, the corrosion depth predicted by this model converges to the pre-set long-term corrosion wastage value. Other models are summarised in the authors' review paper [2]. Only regression models proposed by Guedes Soares et al. [54,54] and Zayed et al. [55] explicitly account for environmental factors. Guedes Soares et al. defines relationships between corrosion rate and temperature, flow velocity and dissolved oxygen for structures

Table 1
Test environments and methods used for immersion and atmospheric corrosion studies.

		Immersion corrosion‘	Atmospheric corrosion
Test environment	Laboratory	[3–6,8,10,11,13–26,28–31]	n/a
	Field (coastal/harbour)	[3,9,24–26]	[21–23,27–42]
Test method	Weight loss	[1,2,6–8,10–12,19,26]	[32–41,43–49]
	Electrochemical	[7,46–49]	n/a
	Combined	[5,8,11–20,50,51]	[34,35]

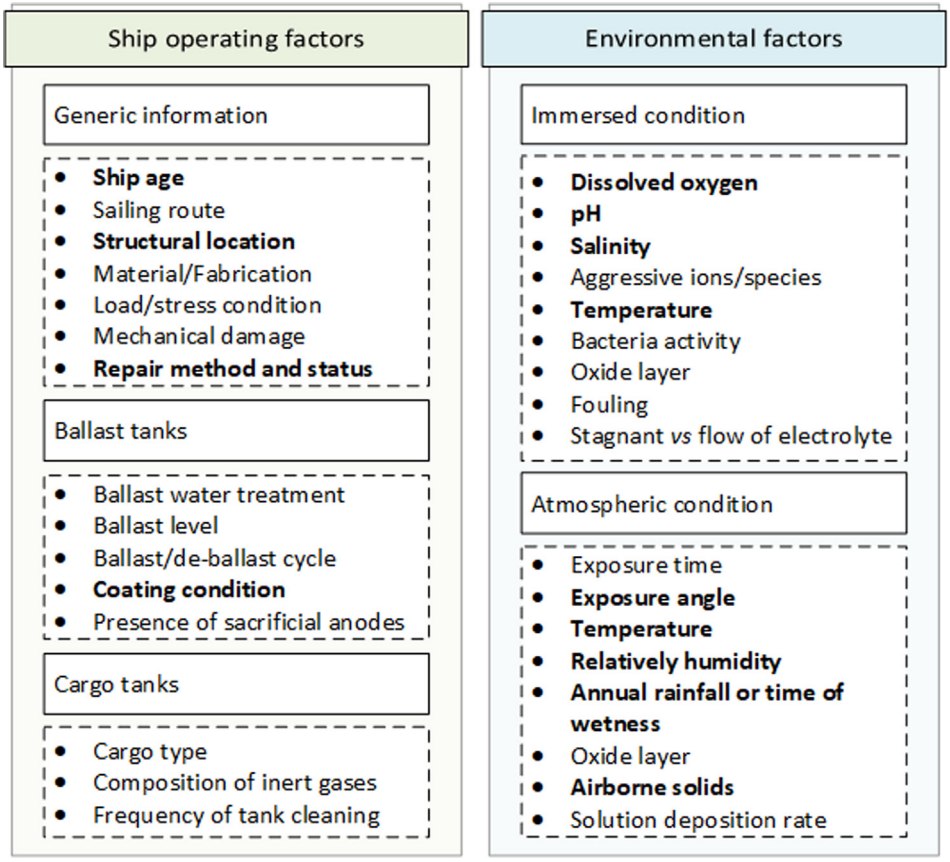

Fig. 1. Key factors influencing ship corrosion (factors highlighted in bold are explicitly incorporated into the proposed model).

immersed in seawater [53] and the relative humidity and chloride concentration are incorporated for atmospheric corrosion [54]. Zayed et al. [55] divided ship structures into different environmental regions and used the corresponding corrosion wastage allowance of each region from the IACS Harmonised Common Structural Rule (CSR-H) to calibrate the Guedes Soares and Garbatov model [56]. However, the accuracy of these regression models is not clear and a number of key environmental factors are not included.

To account for the multi-variate nature of marine corrosion, machine learning methods are increasingly implemented to predict the corrosion rate [58–68] and corrosion depth [70,70]. These methods are also used to identify the corrosion type in seawater or marine atmospheric conditions [69,71–73]. These models provide accurate prediction results, with the coefficient of determination (R^2) above 0.8 and more than 95% accuracy in recognition of the corrosion type. The most frequently used machine learning methods are Artificial Neural Networks (ANNs) for regression problems and Support Vector Machines (SVMs) for classification problems. The number of data that the approaches were used for ranges between 46 and 6540 with most of the data taken from laboratory experiments. Although these approaches show promising predictions of the thickness reduction in steels due to corrosion, the scope of applications is limited to the associated experiments rather than actual usage for ships.

This paper proposes an ANN-based data fusion approach using ship survey thickness measurements (TM) and corrosion experimental data to provide tailored corrosion predictions for sweater ballast tanks and decks of bulk carriers. The goal is to capture a wider range of influencing factors (both operational and environmental), as highlighted in bold in Fig. 1, in the corrosion prediction process and to investigate the resulting method approximation of the fundamental understanding of marine corrosion mechanisms. The ship survey thickness measurement dataset was collected from periodical surveys of 44 vessels from 9.75-year-old to 25.25-year-old, containing 2978 measurements from six structural locations, and complimented with experimental data sourced from the literature, containing 253 measurements. The approach is compared with two representative empirical models and a traditional ANN model based solely on the TM data. A sensitivity analysis was subsequently carried out to understand the influence of each input variable on the corrosion behaviour. The prediction was also compared with current design requirements of corrosion allowances.

2. Methodology to predict corrosion from a fusion of datasets

An important factor in this prediction is the ability to represent the physics or fit to the ground truth. Existing machine learning approaches to achieve this can be divided into four categories. The first category is modifying the loss function, which is normally based on the Minkowski family of error metrics, by using physical rules when solving regression problems [75–76]. However, it is difficult to find a simplified equation to quantify marine corrosion due to its multi-variate nature, Fig. 1. The second category is to pre-train an ANN with data from models that represent the base/-partial physical relationships between inputs and outputs. This biases the network's weights to this relationship and allows the operational data to adjust this representation to the available data [77]. However, this method is also not applicable in this case due to the lack of suitable corrosion models. In the third category, the kernels within nodes of the machine learning approach are adapted to force the network to follow a predefined response [78]. While this approach is effective it is difficult to adapt and the most beneficial kernel needs recalculating/recalibrating as the approach is improved. Finally, a fusion of different datasets can be used where some data represents the fundamental relationships which augment the data from operation, allowing a more general use of the network [72,79]. This data fusion concept was selected and the model architecture is illustrated in Fig. 2. The inputs and outputs are summarised in Table 2 and the three parts of the model (represented by three colours in Fig. 2) are detailed in the following subsections.

2.1. ANN model based on ship survey TM data (ANN model 1)

Several ship survey TM datasets were reviewed [53,80–83]. The data from Paik et al. [80] was selected to develop the model because it contains the highest number of variables and measurements compared with the other datasets, with measurements from eight structural locations of seawater ballast tanks and decks. These were collected from 44 bulk carriers, aged between 9.75 and 25.25 years old. Each measurement was obtained by averaging several thickness readings within a plate [80] and the raw data is shown in Fig. 3. The ship survey TM dataset contained 2203 data points by only keeping data from structures that are either immersed in seawater: outer bottom plates, lower wing tank side shells and side shells; and the structures that are exposed to marine atmospheric environments: upper wing tank side shells, upper sloping plates and upper deck plates. To fuse the ship survey thickness measurements with the experimental data, corrosion depths in Fig. 3 were converted to corrosion rates, assuming that corrosion started after five years of service [81,81].

The measurements cannot be linked to individual ships, making it difficult to accurately trace the corrosion behaviour at each structural location, and the operating factors listed in Fig. 1 cannot be traced to individual ships either. The database was imbalanced, with different data densities in different regions. Table 3 shows that the majority of the data ranges between 0 and 0.15 mm/year. The data was also discontinuous, as seen in Fig. 3, due to the data being collected at periodical surveys. To have a more evenly distributed dataset for better regression performances, the data was transformed to a symmetrical distribution, using Eq. (1),

$$X = arc\sinh\sqrt{x} \tag{1}$$

where x is the original corrosion rate and X is the adjusted corrosion rate, both in mm/year. This function was chosen since it shows the best performance in improving the correlation between the inputs and outputs when comparing several functions commonly used for transforming data [84].

Due to the rather limited information in the TM dataset, an additional supervised machine learning algorithm, the SVM for multi-class classification [85], was utilised to classify the data into three corrosion levels. These are minor, moderate and severe corrosion, which were defined using 10% and 90% cumulative probability of corrosion rate, correlating with the definitions in the CSR-H. Since the ship survey TM reports indicate the renewal status of each measured structural component, the renewal status of each data in this paper was estimated. This was based on the assumption that if there was no data between 0 and 0.5 mm for two consecutive half-year time periods, and the corrosion depth was 0 mm at the following time point, this time point was considered to be a renewal.

The ANN model 1 (yellow branch in Fig. 2) has four layers, including one input layer, two hidden layers and one output layer. The model was built using Keras 2.3.1 and Tensorflow 2.1.0. It was trained on the TM data. Each hidden layer in the ANN had 32 neurons, selected after performing a parametric study from 8 neurons to 64 neurons, and was trained using a 20% dropout rate to minimise overfitting based on the stochastic nature of the data. This

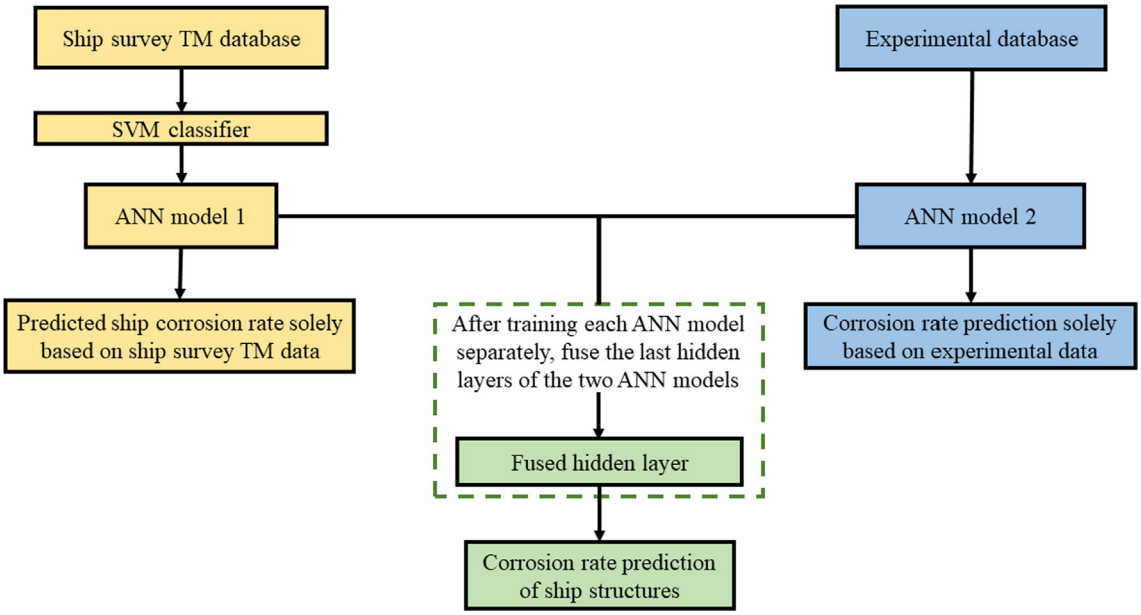

Fig. 2. The data fusion network architecture, with the ship survey data trained network (ANN model 1) in yellow, experimental data trained network (ANN model 2) in blue, and a fused layer in green to combine the predictions. (For interpretation of the references to colour in this figure legend, the reader is referred to the web version of this article.)

Table 2
Inputs into the different networks.

Ship survey TM database		Experimental database	
Structural type	Inputs	Corrosion type	Inputs
Immersed structures	• Ship age • Structural location • Corrosion level • Renewal status	Immersion corrosion	• Temperature • pH • Salinity • Dissolved oxygen
Structures exposed to marine atmospheric environments	• Ship age • Structural location • Corrosion level • Renewal status	Marine atmospheric corrosion	• Temperature • Relative humidity • Annual rainfall • Chloride deposition rate • SO_2 deposition rate

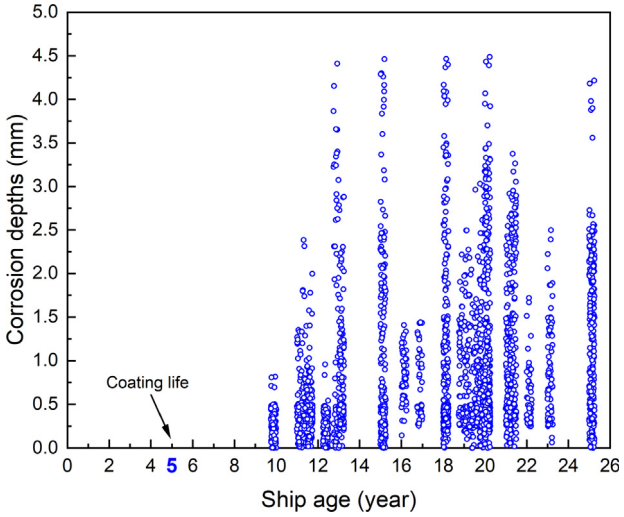

Fig. 3. Corrosion data from 44 bulk carriers at eight ballast tank structural locations, where the coating life is documented as being 5 years on average [80].

means that 20% of the 32 neurons were randomly deactivated during training, ensuring that the training of the weights was protected against extreme values. Fig. A1 in the Appendix indicates the convergence at 32 neurons when tested from 8 neurons to 64 neurons. Due to its performance on avoiding saturation [86], the 'Relu' (Rectified Linear Unit) activation function was used in the hidden layers and a linear activation function was implemented in the output layer. An adaptive learning rate optimisation algorithm, 'Adam', was implemented to train the ANN. The batch size was set to 32 after a small parametric study and the epoch number was set at 1000. The hyperparameters of the ANN model are summarised in Table 4.

To verify the performance of the model, all data in the databases were randomly split into a training data set (70%), a validation data set (10%) and a testing data set (20%). The validation data was used at the end of every epoch to determine the accuracy of the model. Early stopping was applied in the training process where if the loss was stable for 100 epochs, it was terminated. The testing data was used after the training was complete to determine the accuracy of the model. Since the initial weights of the ANN were randomly generated, and the data used for training were randomly selected, the model was independently trained for 30 times for robustness. The prediction error and the proportion of variance in the predicted corrosion rate were evaluated using the mean absolute error (MAE), root mean squared error (RMSE) and the R^2. In general, a low MAE and RMSE as well as a high R^2 value indicate an accurate prediction.

2.2. ANN model for the experimental data (ANN model 2)

The experimental database was taken from various literature and contained 188 corrosion rate measurements of mild and high

Table 3
Determination of the skewness of the ship survey thickness measurement dataset.

Corrosion rate range [mm/year]	Percentage of thickness measurement in the dataset		Percentage of thickness measurement after transformation	
	Immersed structures	Structures above seawater	Immersed structures	Structures above seawater
0–0.05	62.4%	60.4%	1.7%	1.4%
0.05–0.15	33.3%	31.8%	23.8%	20.9%
0.15–0.30	3.2%	7.6%	59.7%	60.9%
0.30–0.50	1.7%	0.3%	13.7%	16.4%
>0.50	0.1%	0%	1.2%	0.4%

Table 4
The hyperparameters of the ANN model.

Hyperparameter	Value
Number of hidden layers	2
Number of neurons in each hidden layer	32
Batch size	32
Number of epochs	1000
Early stopping patience	100
Error function	Mean absolute error (MAE)
Optimiser	Adam
Learning rate	0.01
Activation function	Relu
Dropout rate	0.2
Initialiser	Random

strength carbon steels (H32 and H36) in fully immersed seawater conditions [44,45,48,49] and 65 measurements of carbon steels in marine atmospheric conditions [29,32,36,37]. The experimental data were mostly obtained using the weight loss method following the ASTM G1-03 standard. The immersion corrosion experimental data were obtained after 14–68 days of immersion. The marine atmospheric experimental data were obtained after an exposure of 1–5 years. The experimental database of immersion corrosion was filtered to the range of global seawater statistics, leaving 77 measurements, as shown in Table 5. All collected marine atmospheric corrosion experimental measurements were kept since they are all from field tests.

The ANN architecture to regress the experimental data had two hidden layers and 32 neurons in each layer, selected after performing a parametric study (Fig. A1). The same activation function as for the ANN model 1 was used in the hidden layers and the output layer. The model also used the same dropout rate, data set splitting method and optimisation algorithm as for the ANN model 1. The batch size was set to 16, selected after a small parametric study, and the epoch number was set as 1000. Early stopping of 100 epochs was applied to the training process. The model was independently trained for 30 times, using the same metrics as the previous study. After training on the experimental database, a sensitivity analysis was performed to quantify the influence of each input variable on the corrosion rate by using the partial derivative method [88,88].

2.3. ANN with data fusion of ship survey TM and the experimental datasets

The model representing the ship survey TM dataset was fused with the model representing experimental data from the marine immersion or atmospheric corrosion conditions. The network architecture of the ANN after data fusion is shown in Fig. 4. As the experimental input variables were different to the ship survey thickness measurement dataset, the fusion layer combined the two through three ship survey input variables, namely the environment temperature, the structural location and the corrosion level, as illustrated in Table 2. As the sailing route information was not available from the database, the environmental temperature was determined according to the temperature values provided by Guedes Soares et al.'s temperature-corrosion rate empirical models [54,54], as listed in Table 6. Gaussian noises, with a mean value of 0 °C and a standard deviation of 1 °C, were added to each temperature value generated from the empirical models. The ship survey TM data was matched to a corresponding corrosion experimental data point by finding the same or similar temperature, defined based on a temperature difference of within ± 0.5 °C between the TM data and experimental data. The structural locations were used to determine the corrosion type, i.e., marine atmospheric corrosion or immersion corrosion. Depending on the corrosion level, severe, moderate or low, the experimental input variables corresponding to the highest, median or the lowest corrosion rate were utilised.

The proposed data fusion model was compared to the model solely based on ship survey TM database (ANN model 1). The same training process as used in the ANN model 1 was implemented, using 70% of data as training data set, 10% of data as validation set and 20% of data as testing data set. The training was repeated for 30 times, using the same metrics as the ANN model 1.

3. Results and discussion

3.1. Predictions based on ship survey TM data

The prediction results of the testing dataset from the ANN model 1 (based on the ship survey TM data) are shown in Fig. 5. These are from the best case with the lowest MAE from the 30

Table 5
The range of factors in the experimental database and the global seawater statistics.

		Experimental database	Global seawater [53]
Immersion corrosion experiments	Seawater temperature (°C)	0–35 (Mean 23.5)	−2–35 (Mean 15.5)
	Dissolved oxygen (mg/L)	4–12 (Mean 6.8)	4–10.4 (Mean 5.9)
	Salinity (ppt)	24–43 (Mean 32.2)	27–40 (Mean 34.3)
	pH value	6–9 (Mean 7.7)	7–8.4 (Mean 8.2)
Marine atmospheric corrosion experiments	Annually average temperature (°C)	11.3–32 (Mean 23.1)	
	Relative humidity (%)	50–93 (Mean 70.1)	
	Average annual rainfall (mm/year)	58.5–9908 (Mean 1259)	
	Chloride deposition rate (mg/m^2/day)	3.8–968.3 (Mean 140.7)	

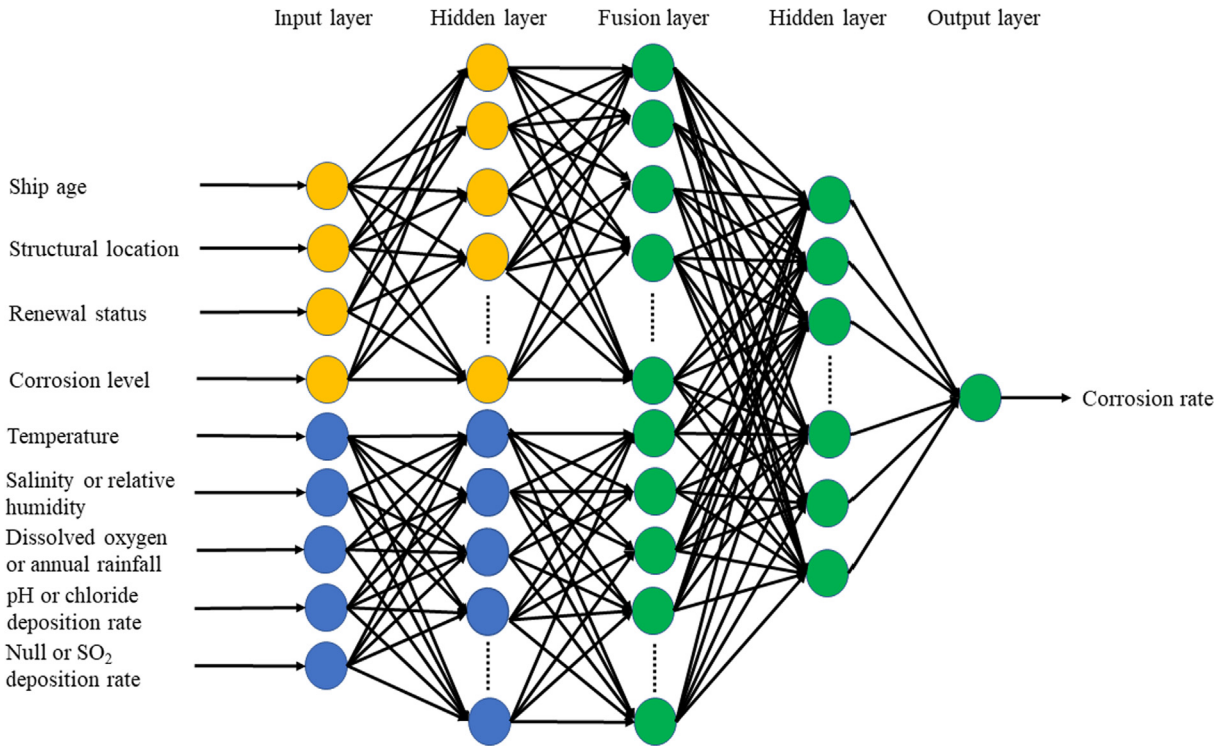

Fig. 4. The ANN network architecture for the data fusion model.

Table 6
Estimated temperatures for the dataset.

Measured ship structural component	Mean temperature	Standard deviation
Outer bottom plates	11 °C	3.9 °C
Lower wing tank side shells	13 °C	5.1 °C
Side shells	20 °C	1.9 °C
Upper wing tank side shells	19 °C	1.0 °C
Upper sloping plates	21 °C	1.1 °C
Upper deck plates	20 °C	1.0 °C

independent trainings. It can be seen that the predictions are skewed to the left in both environmental conditions. This is because the ANN tends to fit to the values with a high data density, with corrosion depths lower than 0.5 mm. Hence, it underestimates the higher corrosion depths. The use of SVM to classify the corrosion levels and normalisation of the data, detailed in Section 2.1, reduce the skewness to some extent. However, it cannot fully resolve the imbalanced nature of the dataset. The 2σ values, representing the two standard deviations of all markers' errors (error = actual value – predicted value), are 0.75 mm for immersed

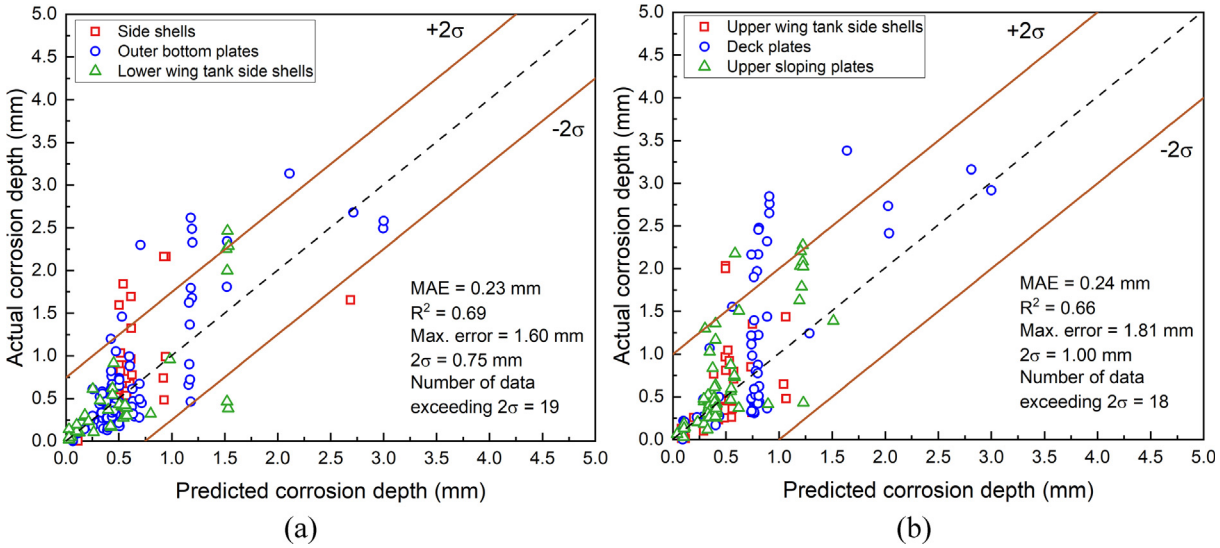

Fig. 5. Prediction results of the ANN model 1 based on ship survey TM data: (a) the immersed structures (b) the structures above seawater.

structures and 1.00 mm for the structures above seawater. The number of outliers, which are the markers exceeding the 2σ boundaries for the two structural conditions are 19 and 18, respectively. Most of these data points have actual corrosion depth higher than 0.5 mm. The mean values (and standard deviations) of the MAEs from the 30 independent trainings are 0.27 mm (0.02 mm) for immersed structures and 0.28 mm (0.02 mm) for the structures above seawater. For the RMSE, the mean values (and standard deviations) are 0.46 mm (0.04 mm) for the immersed structures and 0.47 mm (0.04 mm) for the structures above seawater. The mean (and standard deviations) of R^2 values are 0.55 (0.08) and 0.48 (0.1) for each environmental condition.

3.2. Predictions from data fusion of ship survey TM and experimental data sets

The prediction results of the testing dataset from the data fusion model are shown in Fig. 6, representing the best case with the lowest MAE from the 30 independent trainings. It can be seen that the markers are much closer to the diagonal line compared to Fig. 5, with the 2σ values reduced by approximately 50%. The number of data points exceeding the 2σ boundaries are similar in Fig. 5 (a) and Fig. 6(a). However, this number is reduced from 18 to 4 by using the data fusion model for structures above seawater. The skewness is significantly reduced for the corrosion depth below 2 mm, compared with the predictions from ANN model 1 (Fig. 5). The 30 independent trainings resulted in an average MAE (and standard deviations) of 0.15 mm (0.02 mm), reduced by 44%, for the immersed structures and 0.13 mm (0.01 mm), reduced by 54%, for structures above seawater. The mean values (and standard deviations) of RMSE are 0.38 mm (0.04 mm), reduced by 17%, for the immersed structures and 0.24 mm (0.03 mm), reduced by 49%, for the structures above seawater. The mean values (and standard deviations) of R^2 are 0.69 (0.09), increased by 25%, for the immersed structures and 0.87 (0.04), increased by 81%, for the atmospheric condition. Furthermore, the robustness of the pro-

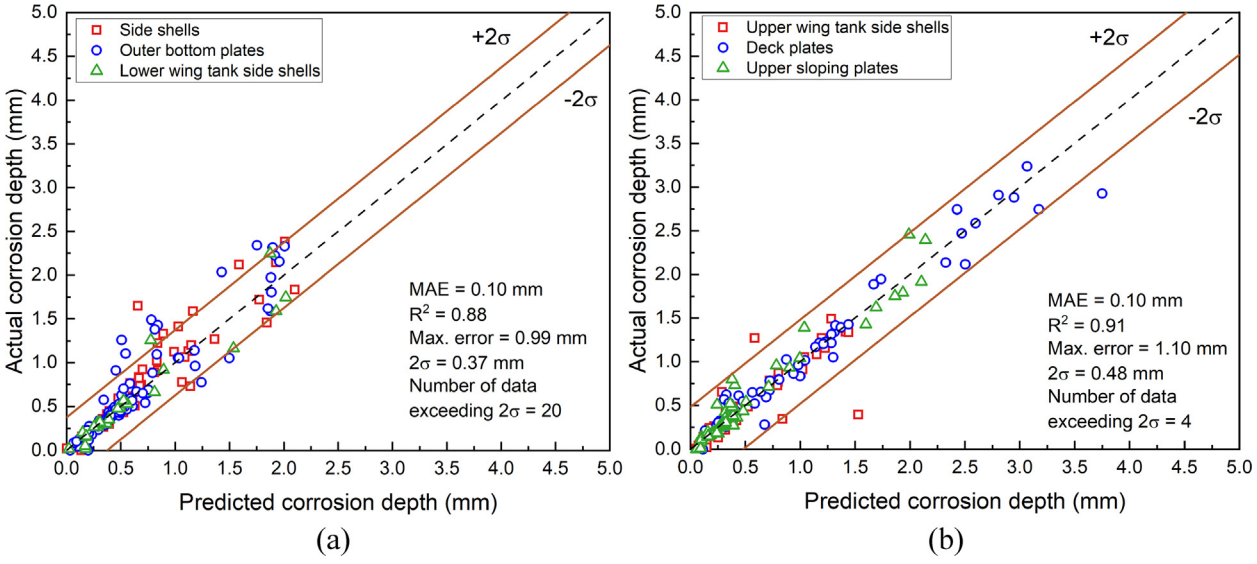

Fig. 6. Prediction results from a fusion of experimental and TM data: (a) the immersed structures (b) the structures above seawater.

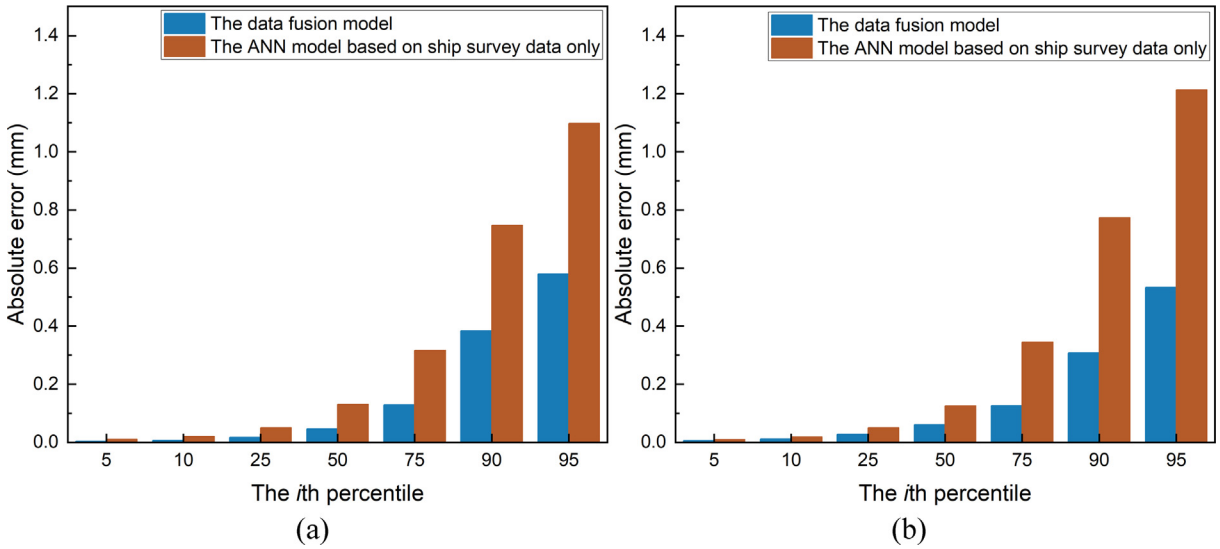

Fig. 7. Percentiles of prediction absolute error from the two models: (a) the immersed structures (b) the structures above seawater.

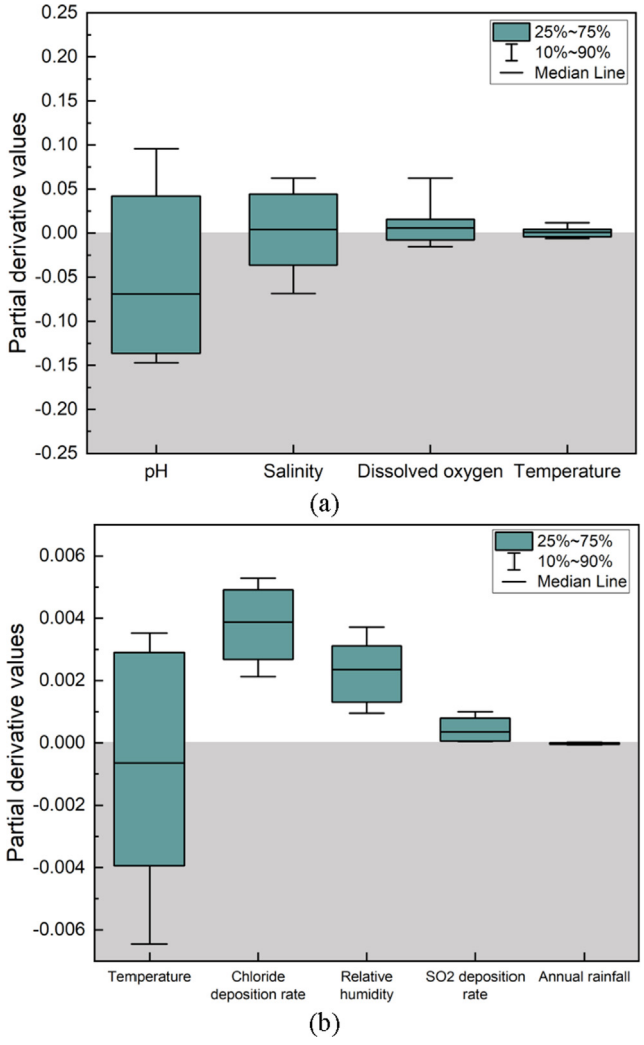

Fig. 8. Sensitivity of each input variable on the (a) immersion and (b) atmospheric marine corrosion rates of carbon steels.

posed model for the structures above seawater is also improved with smaller standard deviations of the MAE, RMSE and R^2 from all trainings.

The absolute errors between the predicted and actual corrosion depths for all of the 30 independent trainings are shown in Fig. 7. The value at the *i*th percentile represents that *i*% of the values are lower than the *i*th percentile value. It can be seen that the absolute errors of the data fusion model are lower than the ANN model based on ship survey TM data at each percentile. For the data fusion model, 95% of the prediction errors are lower than 0.58 mm for the immersed structures and 0.53 mm for the structures above seawater.

3.3. Sensitivity analysis

The sensitivity analysis of the experimental data is shown in Fig. 8. All the data, including both training and testing dataset, from the experimental database were used to calculate the partial derivatives, which indicates how the corrosion rate changes with an increase of each input variable. These values are taken from the 10th percentile to the 90th percentile to understand how the sensitivity changes within the database. The distribution of percentile markers indicates the importance of the input variable, where the closer the percentile markers are to the zero line the less influential the variable is.

The general influence of each input variable for the immersion corrosion experiments matches well with the results from Paul [48]. Paul stated that the corrosion rate is increased with increased temperature, dissolved oxygen or salinity, whereas increasing pH values from 4 to 8 reduces the corrosion rate. The sensitivity analysis demonstrates the same phenomenon for values under 75th percentile (pH from 6 to 8), showing that increased pH leads to a reduced corrosion rate. This is due to the enhanced formation of calcareous scales on steels in seawater, which provides a level of protection for the metal substrate [61,89]. As the pH increases from 6 to 8, the tendency of the immersion corrosion rate reduction is also decreased. The quantified contribution of each input variable was compared with the feature importance analysis conducted by Diao et al. [60] based on 105 coupon tests. They found the salinity and pH values are the most important environmental

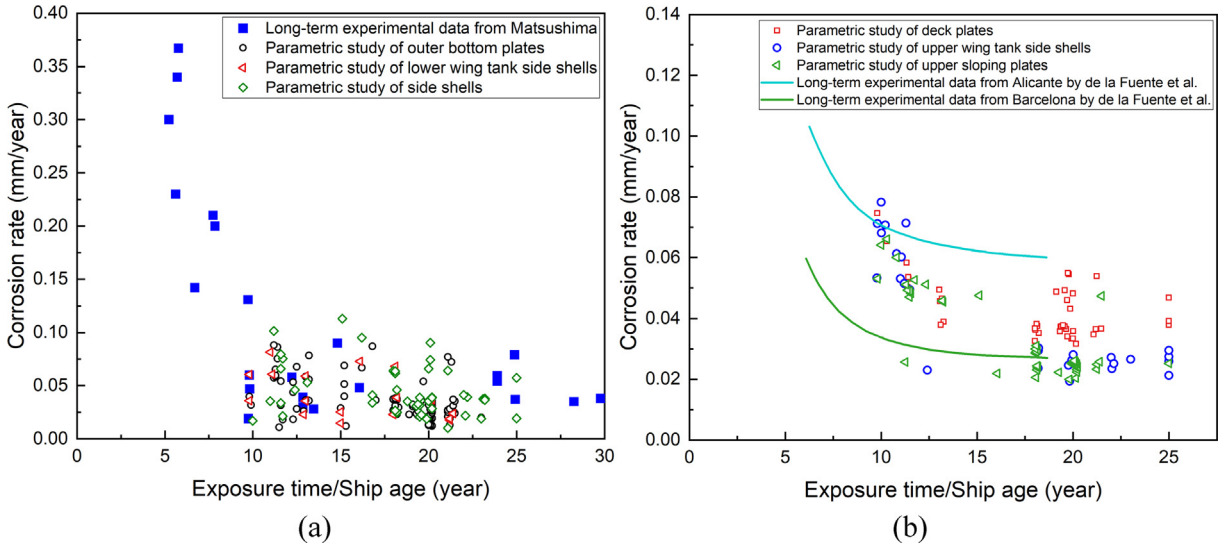

Fig. 9. Influence of the ship age on corrosion rate using the proposed model: (a) Immersed structures compared with data from Matsushima [91]; (b) Structures above seawater compared with data from de la Fuente et al. [41].

factors affecting the immersion corrosion rate. Furthermore, the dissolved oxygen had a slightly higher effect on the corrosion rate compared to temperature. These findings are confirmed through the current sensitivity analysis, Fig. 8(a). The rate of carbon steel corrosion in seawater is controlled by the rate of dissolved oxygen supply to the metal surface. For the most range of dissolved oxygen, the increased dissolved oxygen results in increased corrosion rate. This, in turn, is determined by the dissolved oxygen concentration in the bulk solution, salinity, temperature and the state of surface filming. Increased temperature will lead to enhanced metal surface activity and the diffusion coefficient of oxygen [89] but higher salinity will result in lower oxygen solubility. From Fig. 8 (a) it reveals that the role of salinity is more important and is also more uncertain, or complex, than that of temperature. There are possibilities that salinity can have either a positive or a negative effect on the corrosion rate change. The sensitivity analysis demonstrates that the corrosion rate is increased when the temperature is higher than 22 °C and salinity changing from 24 ppt to 32 ppt. The increased dissolved oxygen concentration enhances the cathodic reaction rate [48] and facilitates the formation of the oxide layer on low-alloy steels [60], which hinders the corrosion process. However, certain combinations of temperature, salinity and dissolved oxygen may also lead to decreased corrosion rate, which is also reported by Paul [48]. In comparison, the pH value has a more definitive effect.

For the marine atmospheric corrosion, the influences of each input variable shown in Fig. 8(b) are in good agreement with the results reported by Zhi et al. [63,65] and Yan et al. [88]. Specifically, the temperature, chloride deposition rate and relative humidity play the most significant roles in the determination of corrosion rate whereas the SO_2 deposition rate and annual rainfall have the least effects. When the temperature is higher than 21 °C, an increased temperature reduces the atmospheric corrosion rate, which is also reported by Refs. [63,65,88]. This is because the increased temperature accelerates the evaporation of the electrolyte film on the steel surface [62]. Furthermore, Castaneda et al. [90] observed that the increased temperature significantly reduces the chloride deposition rate and hence slows down the corrosion rate. However, a positive correlation between temperature and the corrosion rate is reflected in Fig. 8(b) at lower temperature values. Furthermore, the sensitivity analysis demonstrates that when annual rainfall is higher than 1457 mm/year, the increased annual rainfall decreases the corrosion rate. This phenomenon was also reported by Zhi et al. [65], where they found the corrosion rate starts to decrease when the rainfall is over 147 mm/month (annual rainfall = 1764 mm/year).

The influence of ship age on the corrosion rate is also examined, where the structures are assumed to be without renewal and under the moderate corrosion level. The parametric study results are compared with field/experimental data collected from the literature Specifically, the experimental data collected by Matsushima were measured at many locations throughout the world and the coupon specimens were immersed for periods from less than 1 year to 40 years [91]. de la Fuente et al. reported the corrosion rate of mild steels with 1–14 years of exposure at marine atmospheric test sites in Alicante and Barcelona [41]. As shown in Fig. 9 (a), for the three immersed structural locations, the predicted corrosion rate lies within Matsushima's data for the time period of 10–25 years and does not change significantly with time. The parametric study results of the three structures above seawater are comparable with the field measurements, with a slight decrease in corrosion rate with increasing exposure time. The same trend can be observed from all of the three structures. In Fig. 9 (b), the deck plate has higher corrosion rate for the ship age between 20 and 25 year-old when compared to the upper wing tank side shells and the upper sloping plates. This indicates that the environmental condition of the deck plates is more complicated, with additional influences from greater temperature fluctuations, splash seawater and possible mechanical damage. The corrosion rate plateaus in long term services, however, the corrosion evolution over time cannot be traced for individual structural component due to the lack of information in the survey TM dataset.

3.4. Comparison with empirical approaches and design requirement

The newly proposed ANN model with data fusion was compared with the state-of-the-art corrosion models proposed by

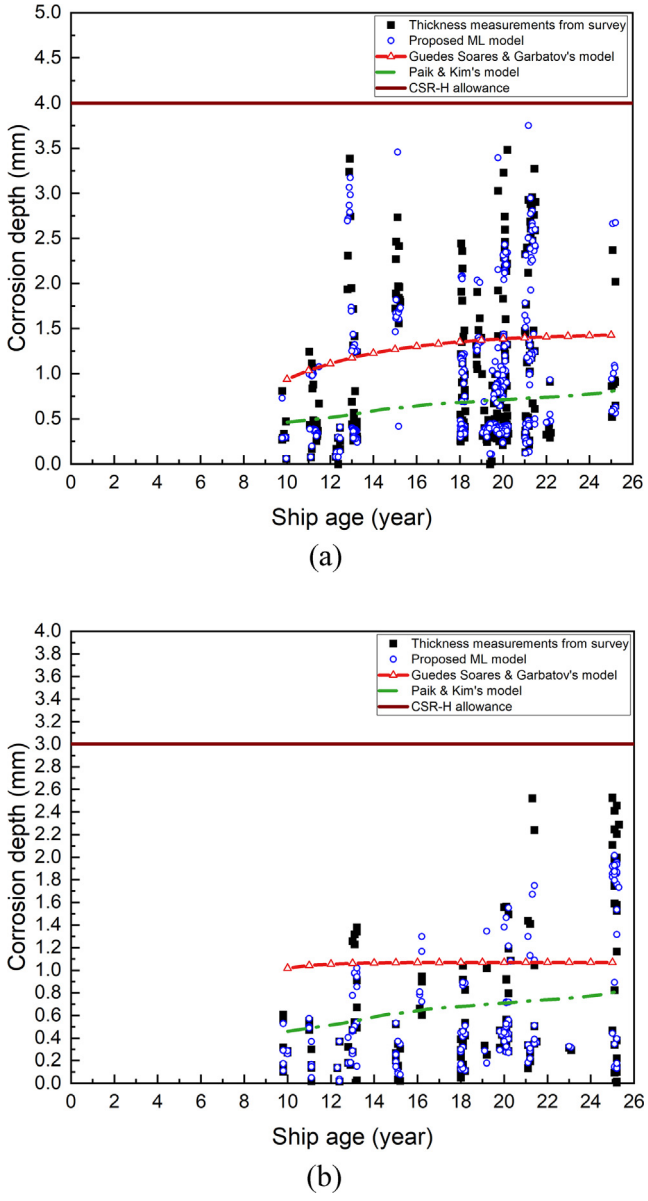

Fig. 10. Comparisons between the actual corrosion depths, the CSR-H allowance, predictions from the proposed model and two representative empirical models for (a) deck plates (Guedes Soares & Garbatov's model: 1.45 mm for the long-term corrosion depth and 4.8 years for the transition time under average condition [2]) and (b) lower wing tank side shells (Guedes Soares & Garbatov's model: 1.07 mm and 1.64 years [92]).

Guedes Soares and Garbatov [56] and Paik and Kim [52]. Guedes Soares and Garbatov's model [56] requires the long-term corrosion wastage, the transition time between coating durability and corrosion initiation and the coating life for the individual structural locations on ships. Paik and Kim [52] provide shape and scale parameters specifically for modelling bulk carriers [52]. These parameters are listed in the caption of Fig. 10 and Table A1 in the Appendix. The comparison of the deck plates and the lower wing tank side shells are shown in Fig. 10. The prediction results of the other structures are listed in Table A1 in the Appendix. The actual corrosion depth from the TM data and the CSR-H design corrosion allowance are also included in the figures. It needs to be noted that the TM dataset is collected from pre-CSR-H ships which may have different designed corrosion allowances. However, the development of CSR-H was based on data collected from older ships and Fig. 10 is to provide some generic understanding of the difference between rule requirements and the actual corrosion damage.

The predictions from Guedes Soares and Garbatov's nonlinear model are within the range between 1 mm and 1.5 mm for both the immersed structures and structures above seawater. Predictions from Paik and Kim's model are between 0.4 mm and 0.8 mm and are independent of structural locations. When comparing the data fusion model to the Guedes Soares and Garbatov's nonlinear model, the mean values of MAEs from the 30 independent trainings are reduced by 82% for immersed structures and by 84% for the structures above seawater. The CSR-H corrosion allowances in the design requirement are always conservative, which could lead to overdesigned scantlings and increased lightweight tonnage. Even after 25 years of service the CSR-H retains a safety factor of 1.85 in the upper sloping plates as the best case scenario although this is only 1.05 in the side shells as the worst case scenario. In comparison, the proposed machine learning method is able to provide tailored predictions taking into account additional influencing parameters and the fundamental understanding/measurements of the corrosion processes.

However, some of the extreme high corrosion depths cannot be predicted with the current data fusion model due to the lack of data within the high corrosion depth region (less than 7% of the total 2203 data points are over 2 mm). A majority of the factors effecting corrosion are not documented and the corrosion rate exceeds the corresponding experimental data. However, a margin of 0.6 mm can be added to the predicted value from the data fusion model to gain a 95% confidence. This will enable tailored maintenance strategies and potential service life extensions. It may also help to find a balance point between a reduced design scantling and a more targeted survey, with the current concerns around climate change a 20% reduction in steel could lead to a 9% reduction in power and emissions [93].

4. Conclusions

Corrosion costs the marine industry $80 billion a year [94]. However, it is challenging to predict due to the complex operational environments and the multiple processes/mechanisms that can change the corrosion rate. To accommodate the sparse documentation about the operating conditions and to account for the large range of influencing factors an ANN based data fusion model is developed to better predict the corrosion phenomenon in ballast tanks of bulk carriers. The main findings are summarised as follows:

- A fusion of data is needed for accurate predictions of the corrosion in ships. Using ship survey TM data alone provides a biased prediction towards low corrosion depths. In comparison, the mean value of the Mean Absolute Error from the 30 independent trainings from the proposed method is reduced by at least 40%.
- This improvement in prediction performance also provides an improvement over the current empirical approaches with the Mean Absolute Error reduced by a minimum of 82%.
- The new ANN model provides corrosion depth predictions with a Mean Absolute Error of 0.10 mm in the best cases for both structural conditions.
- The sensitivity analysis quantifies the importance of influencing factors for carbon steel immersion corrosion as: pH > salinity > dissolved oxygen > temperature. The ranking for carbon steel marine atmospheric corrosion is: temperature > chloride deposition rate > relative humidity > SO_2 deposition rate > annual rainfall.
- Compared with the current design rule requirement, the data fusion machine learning approach could lead to a more optimised ship design with lighter scantlings and more targeted surveys.

Declaration of Competing Interest

The authors declare that they have no known competing financial interests or personal relationships that could have appeared to influence the work reported in this paper.

Acknowledgements

The authors would like to thank Mr Joseph Morelos and Mr Leonidas Koukos from Lloyd's Register for their technical guidance and support. The authors also acknowledge the IRIDIS High Performance Computing Facility and associated support services at the University of Southampton, in the completion of this work. The authors acknowledge the funding from EPSRC Impact Acceleration Account, Lloyd's Register Group and the Lloyd's Register Foundation.

Appendix

See Fig. A1.

The equations of MAE, RMSE and R^2:

The equations of MAE, RMSE and R^2 are given in Eqs. (a1)-(a3) as,

$$MAE = \frac{\sum_{i=1}^{n} |y_i - \hat{y}_i|}{n}, \tag{a1}$$

$$RMSE = \sqrt{\frac{\sum_{i=1}^{n} (y_i - \hat{y}_i)^2}{n}}, \tag{a2}$$

$$R^2 = 1 - \frac{\sum_{i=1}^{n} (y_i - \hat{y}_i)^2}{\sum_{i=1}^{n} \left(y_i - \bar{y}\right)^2}, \tag{a3}$$

where y_i is the actual value; $\hat{y}_i$ is the predicted value; n is the number of data points and $\bar{y}$ is the mean of the actual values of all data points (see Table A1).

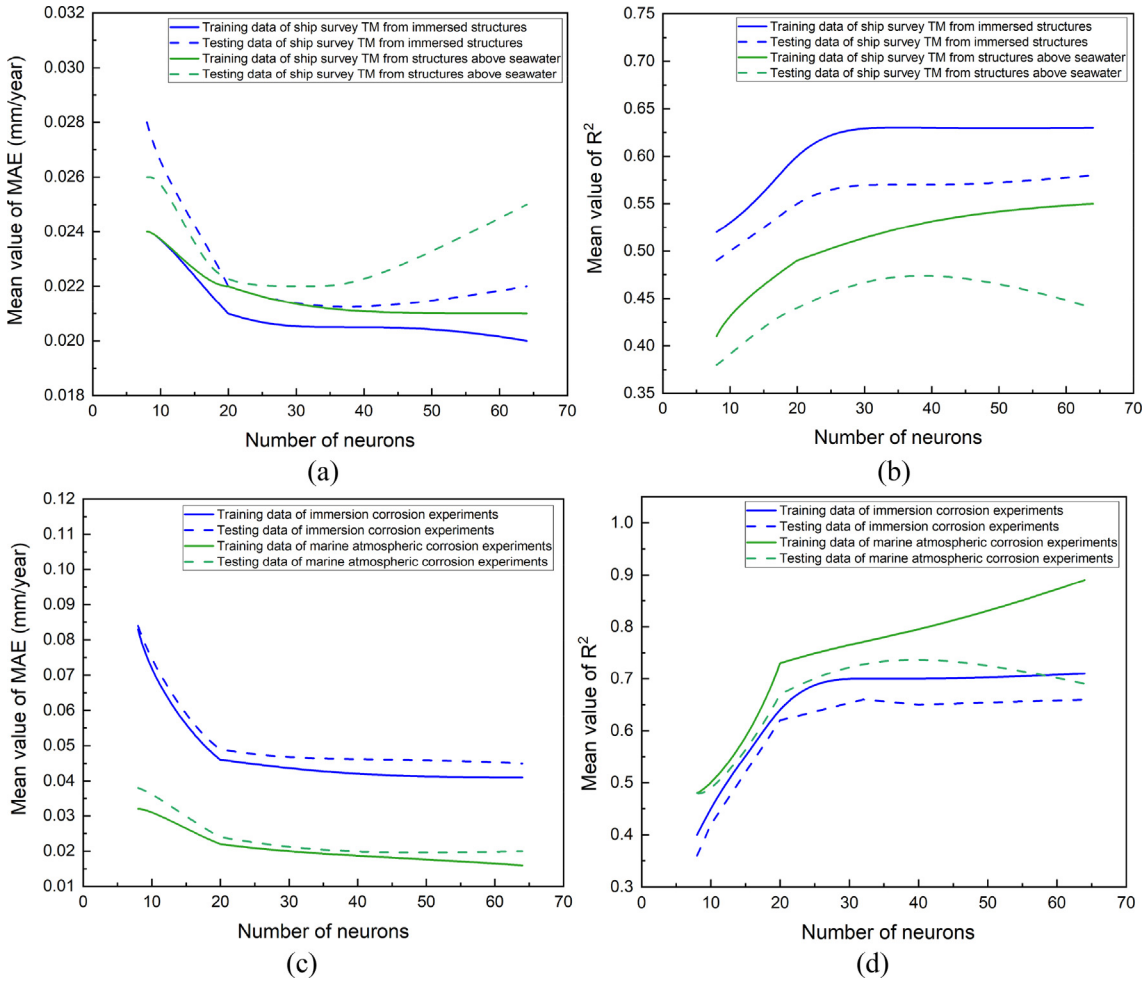

Fig. A1. Convergence of the mean values of MAE and R^2 among 30 independent trainings with increased number of neurons: (a) & (b) from ANN model 1; (c) & (d) from ANN model 2 (both models are indicated in Fig. 2).

Table A1
Comparison between the actual corrosion depths, the predictions from the proposed model and two representative empirical models and the CSR-H allowance.

Structural location	Comparison results
Outer bottom plates (Guedes Soares & Garbatove's model: 1.07 mm for the long-term corrosion depth and 1.64 years for the transition time under average condition)	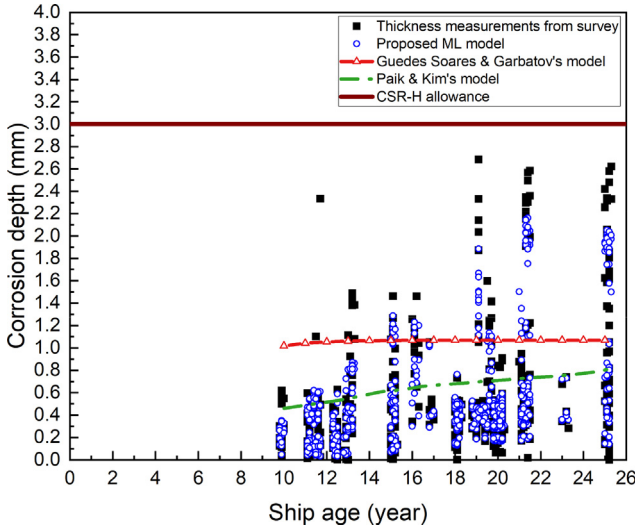

(*continued on next page*)

Table A1 (*continued*)

Structural location	Comparison results
Side shells (Guedes Soares & Garbatove's model: 1 mm and 3.6 years)	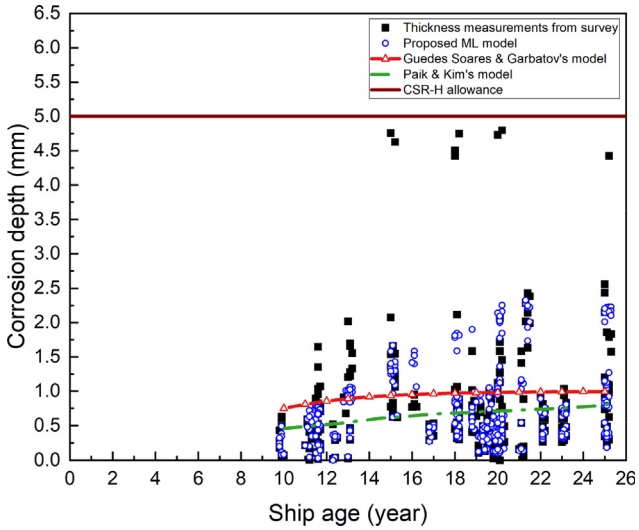
Upper wing tank side shells (Guedes Soares & Garbatove's model: 1 mm and 3.6 years)	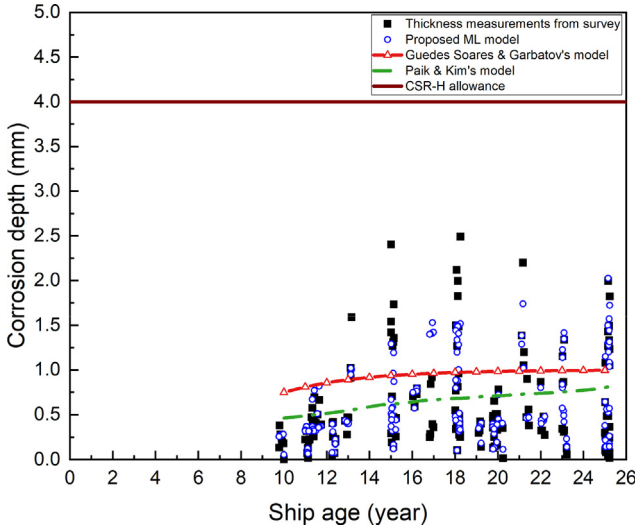
Upper sloping plates (Guedes Soares & Garbatove's model: 1.07 mm and 1.64 years)	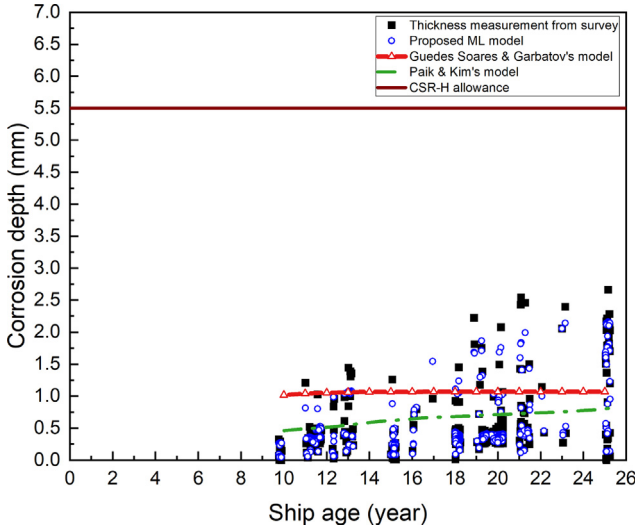

References

[1] H. Ma, X.Q. Chen, R. Li, S. Wang, J. Dong, W. Ke, First-principles modeling of anisotropic anodic dissolution of metals and alloys in corrosive environments, Acta Mater. 130 (2017) 137–146, https://doi.org/10.1016/j.actamat.2017.03.027.

[2] Y. Wang, J.A. Wharton, R.A. Shenoi, Ultimate strength analysis of aged steel-plated structures exposed to marine corrosion damage: a review, Corros. Sci. 86 (2014) 42–60, https://doi.org/10.1016/j.corsci.2014.04.043.

[3] R.E. Melchers, R. Jeffrey, Early corrosion of mild steel in seawater, Corros. Sci. 47 (2005) 1678–1693, https://doi.org/10.1016/j.corsci.2004.08.006.

[4] J.C. Lin, S.L. Chang, S.L. Lee, Corrosion inhibition of steel by thiourea and cations under incomplete cathodic protection in a 3.5% NaCl solution and seawater, J. Appl. Electrochem. 29 (1999) 911–918, https://doi.org/10.1023/A:1003533800038.

[5] Y. Zou, J. Wang, Y. Zheng, Electrochemical techniques for determining corrosion rate of rusted steel in seawater, Corros. Sci. 53 (2011) 208–216, https://doi.org/10.1016/j.corsci.2010.09.011.

[6] P. Refait, A.M. Grolleau, M. Jeannin, C. Rémazeilles, R. Sabot, Corrosion of carbon steel in marine environments: role of the corrosion product layer, Corros. Mater. Degrad. 1 (2020) 198–218, https://doi.org/10.3390/cmd1010010.

[7] J.S. Lee, R.I. Ray, E.J. Lemieux, A.U. Falster, B.J. Little, An evaluation of carbon steel corrosion under stagnant seawater conditions, Biofouling 20 (2004) 237–247, https://doi.org/10.1080/08927010400013274.

[8] J. Liao, K. Kishimoto, M. Yao, Y. Mori, M. Ikai, Effect of ozone on corrosion behavior of mild steel in seawater, Corros. Sci. 55 (2012) 205–212, https://doi.org/10.1016/j.corsci.2011.10.020.

[9] P. Refait, M. Jeannin, R. Sabot, H. Antony, S. Pineau, Electrochemical formation and transformation of corrosion products on carbon steel under cathodic protection in seawater, Corros. Sci. 71 (2013) 32–36, https://doi.org/10.1016/j.corsci.2013.01.042.

[10] Y. Song, K. Dang, H. Chi, D. Guan, Corrosion of marine carbon steel by electrochemically treated ballast water, J. Mar. Eng. Technol. 4177 (2009) 49–55, https://doi.org/10.1080/20464177.2009.11020218.

[11] S. Muralidharan, D.K. Kim, T.H. Ha, J.H. Bae, Y.C. Ha, H.G. Lee, J.D. Scantlebury, Influence of alternating, direct and superimposed alternating and direct current on the corrosion of mild steel in marine environments, Desalination 216 (2007) 103–115, https://doi.org/10.1016/j.desal.2006.11.021.

[12] D.K. Kim, S. Muralidharan, T.H. Ha, J.H. Bae, Y.C. Ha, H.G. Lee, J.D. Scantlebury, Electrochemical studies on the alternating current corrosion of mild steel under cathodic protection condition in marine environments, Electrochim. Acta. 51 (2006) 5259–5267, https://doi.org/10.1016/j.electacta.2006.01.054.

[13] R. Rihan, R. Shawabkeh, N. Al-Bakr, The effect of two amine-based corrosion inhibitors in improving the corrosion resistance of carbon steel in sea water, J. Mater. Eng. Perform. 23 (2014) 693–699, https://doi.org/10.1007/s11665-013-0790-x.

[14] B. Qian, B. Hou, M. Zheng, The inhibition effect of tannic acid on mild steel corrosion in seawater wet/dry cyclic conditions, Corros. Sci. 72 (2013) 1–9, https://doi.org/10.1016/j.corsci.2013.01.040.

[15] J. Wu, D. Zhang, P. Wang, Y. Cheng, S. Sun, Y. Sun, S. Chen, The influence of Desulfovibrio sp. and Pseudoalteromonas sp. on the corrosion of Q235 carbon steel in natural seawater, Corros. Sci. 112 (2016) 552–562, https://doi.org/10.1016/j.corsci.2016.04.047.

[16] K.S. Bokati, C. Dehghanian, S. Yari, Corrosion inhibition of copper, mild steel and galvanically coupled copper-mild steel in artificial sea water in presence of 1H-benzotriazole, sodium molybdate and sodium phosphate, Corros. Sci. 126 (2017) 272–285, https://doi.org/10.1016/j.corsci.2017.07.009.

[17] M. Dehdab, Z. Yavari, M. Darijani, A. Bargahi, The inhibition of carbon-steel corrosion in seawater by streptomycin and tetracycline antibiotics: an experimental and theoretical study, Desalination 400 (2016) 7–17, https://doi.org/10.1016/j.desal.2016.09.007.

[18] K.S. Bokati, C. Dehghanian, Adsorption behavior of 1H-benzotriazole corrosion inhibitor on aluminum alloy 1050, mild steel and copper in artificial seawater, J. Environ. Chem. Eng. 6 (2018) 1613–1624, https://doi.org/10.1016/j.jece.2018.02.015.

[19] B.Y. Liu, Z. Liu, G.C. Han, Y.H. Li, Corrosion inhibition and adsorption behavior of 2-((dehydroabietylamine) methyl)-6-methoxyphenol on mild steel surface in seawater, Thin Solid Films. 519 (2011) 7836–7844, https://doi.org/10.1016/j.tsf.2011.06.002.

[20] X. Luo, X. Pan, S. Yuan, S. Du, C. Zhang, Y. Liu, Corrosion inhibition of mild steel in simulated seawater solution by a green eco-friendly mixture of glucomannan (GL) and bisquaternary ammonium salt (BQAS), Corros. Sci. 125 (2017) 139–151, https://doi.org/10.1016/j.corsci.2017.06.013.

[21] S. Palraj, M. Selvaraj, K. Maruthan, M. Natesan, Kinetics of atmospheric corrosion of mild steel in marine and rural environments, J. Mar. Sci. Appl. 14 (2015) 105–112, https://doi.org/10.1007/s11804-015-1286-x.

[22] M. Morcillo, J.M. González-Calbet, J.A. Jiménez, I. Díaz, J. Alcántara, B. Chico, A. Mazarío-Fernández, A. Gómez-Herrero, I. Llorente, D. de La Fuente, Environmental conditions for akaganeite formation in marine atmosphere mild steel corrosion products and its characterization, Corrosion 71 (2015) 872–886, https://doi.org/10.5006/1672.

[23] J. Alcántara, B. Chico, I. Díaz, D. de la Fuente, M. Morcillo, Airborne chloride deposit and its effect on marine atmospheric corrosion of mild steel, Corros. Sci. 97 (2015) 74–88, https://doi.org/10.1016/j.corsci.2015.04.015.

[24] R. Venkatesan, M.A. Venkatasamy, T.A. Bhaskaran, E.S. Dwarakadasa, M. Ravindran, Corrosion of ferrous alloys in deep sea environments, Br. Corros. J. 37 (2002) 257–266, https://doi.org/10.1179/000705902225006633.

[25] R. Jeffrey, R.E. Melchers, Corrosion of vertical mild steel strips in seawater, Corros. Sci. 51 (2009) 2291–2297, https://doi.org/10.1016/j.corsci.2009.06.020.

[26] X.R. Zhu, G.Q. Huang, L.Y. Lin, D.Y. Liu, Long term corrosion characteristics of metallic materials in marine environments, Corros. Eng. Sci. Technol. 43 (2008) 328–334, https://doi.org/10.1179/147842208X338938.

[27] S.J. Oh, D.C. Cook, H.E. Townsend, Atmospheric corrosion of different steels in marine, rural and industrial environments, Corros. Sci. 41 (1999) 1687–1702, https://doi.org/10.1016/S0010-938X(99)00005-0.

[28] Q.C. Zhang, J.S. Wu, J.J. Wang, W.L. Zheng, J.G. Chen, A.B. Li, Corrosion behavior of weathering steel in marine atmosphere, Mater. Chem. Phys. 77 (2003) 603–608, https://doi.org/10.1016/S0254-0584(02)00110-4.

[29] E. Almeida, M. Morcillo, B. Rosales, Atmospheric corrosion of mild steel Part II – Marine atmospheres, Mater. Corros. 51 (2000) 865–874, https://doi.org/10.1002/1521-4176(200012)51:12<865::AID-MACO865>3.0.CO;2-S.

[30] M. Natesan, S. Selvaraj, T. Manickam, G. Venkatachari, Corrosion behavior of metals and alloys in marine-industrial environment, Sci. Technol. Adv. Mater. 9 (2008), https://doi.org/10.1088/1468-6996/9/4/045002.

[31] C.F. Dong, H. Luo, K. Xiao, Y. Ding, P.H. Li, X.G. Li, Electrochemical behavior of 304 stainless steel in marine atmosphere and its simulated solution, Anal. Lett. 46 (2012) 142–155, https://doi.org/10.1080/00032719.2012.706847.

[32] S. Syed, Atmospheric corrosion of carbon steel at marine sites in Saudi Arabia, Mater. Corros. 61 (2010) 238–244, https://doi.org/10.1002/maco.200905300.

[33] R. Jeffrey, R.E. Melchers, Five year observations of corrosion losses for steels at a severe marine atmospheric site, in: Proc Corros. Prev., 2008, pp. 1–12.

[34] Y. Ma, Y. Li, F. Wang, Corrosion of low carbon steel in atmospheric environments of different chloride content, Corros. Sci. 51 (2009) 997–1006, https://doi.org/10.1016/j.corsci.2009.02.009.

[35] A. Nishikata, F. Suzuki, T. Tsuru, Corrosion monitoring of nickel-containing steels in marine atmospheric environment, Corros. Sci. 47 (2005) 2578–2588, https://doi.org/10.1016/j.corsci.2004.10.009.

[36] M. Natesan, G. Venkatachari, N. Palaniswamy, Kinetics of atmospheric corrosion of mild steel, zinc, galvanized iron and aluminium at 10 exposure stations in India, Corros. Sci. 48 (2006) 3584–3608, https://doi.org/10.1016/j.corsci.2006.02.006.

[37] R. Vera, B.M. Rosales, C. Tapia, Effect of the exposure angle in the corrosion rate of plain carbon steel in a marine atmosphere, Corros. Sci. 45 (2003) 321–337, https://doi.org/10.1016/S0010-938X(02)00071-9.

[38] J.J.S. Rodríguez, F.J.S. Hernández, J.E.G. González, The effect of environmental and meteorological variables on atmospheric corrosion of carbon steel, copper, zinc and aluminium in a limited geographic zone with different types of environment, Corros. Sci. 45 (2003) 799–815, https://doi.org/10.1016/S0010-938X(02)00081-1.

[39] J.G. Castaño, C.A. Botero, A.H. Restrepo, E.A. Agudelo, E. Correa, F. Echeverría, Atmospheric corrosion of carbon steel in Colombia, Corros. Sci. 52 (2010) 216–223, https://doi.org/10.1016/j.corsci.2009.09.006.

[40] Y. Ma, Y. Li, F. Wang, The atmospheric corrosion kinetics of low carbon steel in a tropical marine environment, Corros. Sci. 52 (2010) 1796–1800, https://doi.org/10.1016/j.corsci.2010.01.022.

[41] D. de la Fuente, I. Díaz, J. Simancas, B. Chico, M. Morcillo, Long-term atmospheric corrosion of mild steel, Corros. Sci. 53 (2011) 604–617, https://doi.org/10.1016/j.corsci.2010.10.007.

[42] Z. Wang, J. Liu, L. Wu, R. Han, Y. Sun, Study of the corrosion behavior of weathering steels in atmospheric environments, Corros. Sci. 67 (2013) 1–10, https://doi.org/10.1016/j.corsci.2012.09.020.

[43] R.E. Melchers, Long-term corrosion of cast irons and steel in marine and atmospheric environments, Corros. Sci. 68 (2013) 186–194, https://doi.org/10.1016/j.corsci.2012.11.014.

[44] S.A. Al-Fozan, A.U. Malik, Effect of seawater level on corrosion behavior of different alloys, Desalination. 228 (2008) 61–67, https://doi.org/10.1016/j.desal.2007.08.007.

[45] Z.M. Siddiqi, M.M. Amin, Effect of South China sea water on corrosion behaviour of copper alloy and mild steel, Asian J. Water Environ. Pollut. 14 (2017) 1–8, https://doi.org/10.3233/AJW-170001.

[46] S. Ahmad, A. Malik, Corrosion behaviour of some stainless steels in chloride Gulf seawater, J. Appl. Electrochem. 31 (2001) 1009–1016.

[47] Y. Xu, Q. Zhou, L. Liu, Q. Zhang, S. Song, Y. Huang, Exploring the corrosion performances of carbon steel in flowing natural sea water and synthetic sea waters, Corros. Eng. Sci. Technol. (2020) 1–10, https://doi.org/10.1080/1478422X.2020.1765476.

[48] S. Paul, Model to study the effect of composition of seawater on the corrosion rate of mild steel and stainless steel, J. Mater. Eng. Perform. 20 (2011) 325–334, https://doi.org/10.1007/s11665-010-9686-1.

[49] X. Liu, X. Tang, J. Wang, Correlation between seawater environmental factors and marine corrosion rate using artificial neural network analysis, J. Chinese Soc. Corros. Prot. 25 (2005) 11–14.

[50] W.B.W. Nik, F. Zulkifli, M.M. Rahman, R. Rosliza, Corrosion behavior of mild steel in seawater from two different sites of Kuala Terengganu coastal area, Int. J. Basic Appl. Sci. 11 (2011) 75–80.

[51] H. Möller, E.T. Boshoff, H. Froneman, The corrosion behaviour of a low carbon steel in natural and synthetic seawaters, J. South. African Inst. Min. Metall. 106 (2006) 585–592.

[52] J.K. Paik, D.K. Kim, Advanced method for the development of an empirical model to predict time-dependent corrosion wastage, Corros. Sci. 63 (2012) 51–58, https://doi.org/10.1016/j.corsci.2012.05.015.
[53] C. Guedes Soares, Y. Garbatov, A. Zayed, Effect of environmental factors on steel plate corrosion under marine immersion conditions, Corros. Eng. Sci. Technol. 46 (2011) 524–541, https://doi.org/10.1179/147842209X12559428167841.
[54] C. Guedes Soares, Y. Garbatov, A. Zayed, G. Wang, Influence of environmental factors on corrosion of ship structures in marine atmosphere, Corros. Sci. 51 (2009) 2014–2026, https://doi.org/10.1016/j.corsci.2009.05.028.
[55] A. Zayed, Y. Garbatov, C. Guedes Soares, Corrosion degradation of ship hull steel plates accounting for local environmental conditions, Ocean Eng. 163 (2018) 299–306, https://doi.org/10.1016/j.oceaneng.2018.05.047.
[56] C. Guedes Soares, Y. Garbatov, Reliability of corrosion protected and maintained ship hulls subjected to corrosion and fatigue, J. Sh. Res. 43 (1999) 65–78.
[57] Z. Pei, D. Zhang, Y. Zhi, T. Yang, L. Jin, D. Fu, X. Cheng, H.A. Terryn, J.M.C. Mol, X. Li, Towards understanding and prediction of atmospheric corrosion of an Fe/Cu corrosion sensor via machine learning, Corros. Sci. 170 (2020) 108697, https://doi.org/10.1016/j.corsci.2020.108697.
[58] B.A. Salami, S.M. Rahman, T.A. Oyehan, M. Maslehuddin, S.U. Al Dulaijan, Ensemble machine learning model for corrosion initiation time estimation of embedded steel reinforced self-compacting concrete, Measurement. 165 (2020), https://doi.org/10.1016/j.measurement.2020.108141.
[59] A.Z. Shirazi, Z. Mohammadi, A hybrid intelligent model combining ANN and imperialist competitive algorithm for prediction of corrosion rate in 3C steel under seawater environment, Neural Comput. Appl. 28 (2017) 3455–3464, https://doi.org/10.1007/s00521-016-2251-6.
[60] Y. Diao, L. Yan, K. Gao, Improvement of the machine learning-based corrosion rate prediction model through the optimization of input features, Mater. Des. 198 (2021) 109326, https://doi.org/10.1016/j.matdes.2020.109326.
[61] Y. Lv, J. Wang, J. Wang, C. Xiong, L. Zou, L. Li, D. Li, Steel corrosion prediction based on support vector machines, Chaos Solit. Fract. 136 (2020), https://doi.org/10.1016/j.chaos.2020.109807.
[62] Y. Zhi, T. Yang, D. Fu, An improved deep forest model for forecast the outdoor atmospheric corrosion rate of low-alloy steels, J. Mater. Sci. Technol. 49 (2020) 202–210, https://doi.org/10.1016/j.jmst.2020.01.044.
[63] C.I. Rocabruno-Valdés, J.G. González-Rodriguez, Y. Díaz-Blanco, A.U. Juantorena, J.A. Muñoz-Ledo, Y. El-Hamzaoui, J.A. Hernández, Corrosion rate prediction for metals in biodiesel using artificial neural networks, Renew. Energy. 140 (2019) 592–601, https://doi.org/10.1016/j.renene.2019.03.065.
[64] C. Wang, W. Li, G. Xin, Y. Wang, S. Xu, Prediction model of corrosion current density induced by stray current based on QPSO-driven neural network, Complexity (2019), https://doi.org/10.1155/2019/3429816.
[65] Y. Zhi, D. Fu, D. Zhang, T. Yang, X. Li, Prediction and knowledge mining of outdoor atmospheric corrosion rates of low alloy steels based on the random forests approach, Metals (Basel) 9 (2019), https://doi.org/10.3390/met9030383.
[66] P. Wang, Q. Quan, Prediction of corrosion rate in submarine multiphase flow pipeline based on PSO-SVM model, in: IOP Conf. Ser. Mater. Sci. Eng., 2019, p. 044015. https://doi.org/10.1088/1757-899X/688/4/044015.
[67] C.L.C. Roxas, B.A. Lejano, An artificial neural network model for the corrosion current density of steel in mortar mixed with seawater, Int. J. Geomate. 16 (2019) 79–84, https://doi.org/10.21660/2019.56.4585.
[68] J.S. Chou, N.T. Ngo, W.K. Chong, The use of artificial intelligence combiners for modeling steel pitting risk and corrosion rate, Eng. Appl. Artif. Intell. 65 (2017) 471–483, https://doi.org/10.1016/j.engappai.2016.09.008.
[69] M.E.A. Ben Seghier, B. Keshtegar, K.F. Tee, T. Zayed, R. Abbassi, N.T. Trung, Prediction of maximum pitting corrosion depth in oil and gas pipelines, Eng. Fail. Anal. 112 (2020) 104505, https://doi.org/10.1016/j.engfailanal.2020.104505.
[70] M.J. Jiménez-Come, I.J. Turias, J.J. Ruiz-Aguilar, A two-stage model based on artificial neural networks to determine pitting corrosion status of 316L stainless steel, Corros. Rev. 34 (2016) 113–125, https://doi.org/10.1515/corrrev-2015-0048.
[71] C. Völker, S. Kruschwitz, G. Ebell, A machine learning-based data fusion approach for improved corrosion testing, Surv. Geophys. 41 (2020) 531–548, https://doi.org/10.1007/s10712-019-09558-4.
[72] X. Gong, C. Dong, J. Xu, L. Wang, X. Li, Machine learning assistance for electrochemical curve simulation of corrosion and its application, Mater. Corros. 71 (2020) 474–484, https://doi.org/10.1002/maco.201911224.
[73] Y. Hou, C. Aldrich, K. Lepkova, L.L. Machuca, B. Kinsella, Analysis of electrochemical noise data by use of recurrence quantification analysis and machine learning methods, Electrochim. Acta. 256 (2017) 337–347, https://doi.org/10.1016/j.electacta.2017.09.169.
[74] A. Karpatne, W. Watkins, J. Read, V. Kumar, Physics-guided Neural Networks (PGNN): An Application in Lake Temperature Modeling, 2017. http://arxiv.org/abs/1710.11431.
[75] X. Hu, H. Hu, S. Verma, Z.L. Zhang, Physics-guided deep neural networks for power flow analysis, IEEE Trans. Power Syst. (2020) 1–8. http://arxiv.org/abs/2002.00097.
[76] X. Jia, J. Willard, A. Karpatne, J. Read, J. Zwart, M. Steinbach, V. Kumar, Physics guided RNNs for modeling dynamical systems: a case study in simulating lake temperature profiles, in: Proc. 2019 SIAM Int. Conf. Data Min., 2019, pp. 558–566. https://doi.org/10.1137/1.9781611975673.63.
[77] A.D. Dourado, F. Viana, Physics-Informed Neural Networks for Bias Compensation in Corrosion-Fatigue, in: AIAA Scitech 2020 Forum, 2020. https://doi.org/10.2514/6.2020-1149.
[78] R. Ghiasi, P. Torkzadeh, M. Noori, A machine-learning approach for structural damage detection using least square support vector machine based on a new combinational kernel function, Struct. Heal. Monit. 15 (2016) 302–316, https://doi.org/10.1177/1475921716639587.
[79] W. Mu, M. Rahaman, F.L. Rios, J. Odqvist, P. Hedström, Predicting strain-induced martensite in austenitic steels by combining physical modelling and machine learning, Mater. Des. 197 (2021), https://doi.org/10.1016/j.matdes.2020.109199.
[80] J.K. Paik, S.K. Kim, S.K. Lee, Probabilistic corrosion rate estimation model for longitudinal strength members of bulk carriers, Ocean Eng. 25 (1998) 837–860.
[81] J.K. Paik, A.K. Thayamballi, Y.I. Park, J.S. Hwang, A time-dependent corrosion wastage model for seawater ballast tank structures of ships, Corros. Sci. 46 (2004) 471–486, https://doi.org/10.1016/S0010-938X(03)00145-8.
[82] G. Wang, J. Spencer, H. Sun, Assessment of corrosion risks to aging ships using an experience database, J. Offshore Mech. Arct. Eng. 127 (2005) 167–174, https://doi.org/10.1115/1.1894404.
[83] Technical Background on Corrosion Addition, 2005.
[84] G. Koekemoer, J.W.H. Swanepoel, A semi-parametric method for transforming data to normality, Stat. Comput. 18 (2008) 241–257, https://doi.org/10.1007/s11222-008-9053-3.
[85] T. Wu, C. Lin, R. Weng, Probability estimates for multi-class classification by pairwise coupling, J. Mach. Learn. Res. 5 (2004) 975–1005.
[86] X. Glorot, Y. Bengio, Understanding the difficulty of training deep feedforward neural networks, J. Mach. Learn. Res. 9 (2010) 249–256.
[87] V. Nourani, M.S. Fard, Sensitivity analysis of the artificial neural network outputs in simulation of the evaporation process at different climatologic regimes, Adv. Eng. Softw. 47 (2012) 127–146, https://doi.org/10.1016/j.advengsoft.2011.12.014.
[88] L. Yan, Y. Diao, Z. Lang, K. Gao, Corrosion rate prediction and influencing factors evaluation of low-alloy steels in marine atmosphere using machine learning approach, Sci. Technol. Adv. Mater. (2020) 1, https://doi.org/10.1080/14686996.2020.1746196.
[89] D.A. Shifler, Understanding material interactions in marine environments to promote extended structural life, Corros. Sci. 47 (2005) 2335–2352, https://doi.org/10.1016/j.corsci.2004.09.027.
[90] A. Castañeda, F. Corvo, D. Fernández, C. Valdés, Outdoor-indoor atmospheric corrosion in a coastal wind farm located in a tropical Island, Eng. J. 21 (2017) 43–62, https://doi.org/10.4186/ej.2017.21.2.43.
[91] I. Matsushima, Carbon Steel-Corrosion by Seawater, in: Uhlig's Corros. Handb. Third Ed., 2011: pp. 601–607. https://doi.org/10.1002/9780470872864.ch45.
[92] A.P. Teixeira, C. Guedes Soares, G. Wang, Probabilistic modelling of the ultimate strength of ship plates with non-uniform corrosion, J. Mar. Sci. Technol. 18 (2013) 115–132, https://doi.org/10.1007/s00773-012-0197-7.
[93] Wartsila, Boosting energy efficiency: energy efficency catalogue, in: Energy Effic. Cat. Power R&D, Wartsila, 2009.
[94] S. Chambers, Corrosion costing shipping up to $80bn a year, 2021. https://splash247.com/corrosion-costing-shipping-up-to-80bn-a-year/ (accessed March 15, 2021).